Orientational action of edge dislocations on the director field in antiferroelectric smectic-C_A^* films

P. V. Dolganov,[1] N. S. Shuravin,[1,2] V. K. Dolganov,[1] and Atsuo Fukuda[3]

[1]*Institute of Solid State Physics, Russian Academy of Sciences, Chernogolovka, Moscow Region 142432, Russia*

[2]*Moscow Institute of Physics and Technology, Dolgoprudny, Moscow Region 141700, Russia*

[3]*Trinity College, Department of Electronic and Electrical Engineering, University of Dublin, Dublin 2, Ireland*

(Received 14 October 2016; revised manuscript received 8 January 2017; published 31 January 2017)

We report imaging of the director field near edge dislocations in thermotropic antiferroelecric smectic-C_A^* (SmC_A^*) liquid crystal. Measurements were made in freestanding films with thickness from two to ten smectic layers. We find two different orientations of the molecular tilt plane with respect to the edge dislocation line. The orientation is determined by the value of the Burgers vector of the dislocation. Elementary edge dislocation and dislocations with a Burgers vector equal to an odd number of layers orient the tilt plane perpendicular on the two sides of the dislocation. Dislocations with a Burgers vector equal to an even number of layers orient the molecular tilt plane parallel to the dislocation line. Difference in the orientation for an odd Burgers vector can be attributed to breaking of antiferroelectric symmetry by the edge dislocation.

DOI: 10.1103/PhysRevE.95.012711

I. INTRODUCTION

Dislocations in smectic liquid crystals break the translational symmetry of smectic separating regions with different numbers of molecular layers. Recently, images of edge dislocations and their cores were obtained in ferroelectric smectic-C^* (SmC^*) using cryotransmission electron microscopy [1]. In these measurements the liquid crystal was heated to the isotropic phase and then quenched in liquid nitrogen. Two types of elementary edge dislocations were observed. In the type A dislocation, the core size is of the order of d where d is the smectic periodicity. In the dislocation of the type S, the core extends along the Burgers vector for a distance of about $4d$. Another method which can be employed to investigations of the dislocation structure is atomic force microscopy [2,3]. For fundamental studies and applications it is very important to know how dislocations interact with molecular orientation. This task can be resolved using optical microscopy in reflected light. In spite of the size of the dislocation core being of the order of several nanometers, dislocations in smectic can be visualized using optical methods [4]. Especially easily, edge dislocations can be observed in thin freestanding films using optical microscopy in reflection mode. Due to strong dependence of reflectivity R on film thickness in thin films $R \sim N^2 d^2$ (where N is the number of smectic layers) even elementary edge dislocations with a modulus of Burgers vector $|\boldsymbol{b}| = d$ are easily observed in nonpolarized light as a line between regions with different reflectivity. In tilted smectic phases projections of the long molecular axes (nematic $\mathbf{n}$ director) onto the layer plane form a two-dimensional field of orientational ordering, the so-called $\mathbf{c}$ director [5]. In nonpolar SmC and polar SmC^* phases dislocations not only change the number of smectic layers but also cause parallel orientation of the director field on two sides from the dislocation line. Zhang *et al.* [1] found two types of orientations. In the A dislocation molecular tilt in SmC^* is perpendicular to the dislocation axis. In S type the tilt is parallel to it. Another system was studied by Galerne *et al.* [6,7] in the investigations of layer-by-layer transitions from the isotropic to the Sm-O phase. The structure of the Sm-O is of the herringbone (anticlinic) type (the original name Sm-O was later changed to SmC_A). In their experiments above the isotropic-smectic transition the smectic film floated on the free surface of the droplet that was deposited on the glass plate. When cooled, new layers appear in the smectic film at the smectic-isotropic interface. A layer step between smectic regions with different thickness was interpreted as a surface dislocation line.

Let us first discuss the position of a dislocation in a film. According to existing models [3,8] interaction of the dislocation with the free smectic surface depends on the ratio $\gamma/\sqrt{KB}$, where γ is the surface tension, K is the layer bending constant, B is the bulk compressibility. Typical values of material parameters in liquid crystals with free surfaces correspond to $\gamma/\sqrt{KB} > 1$. In this case the dislocation is repelled from free surfaces and the equilibrium position of the dislocation is in the middle of the freestanding film [8]. On the isotropic-smectic boundary the surface tension γ is small and $\gamma/\sqrt{KB} < 1$. This can be the reason that in the droplets the dislocation locates on the isotropic-smectic surface. Galerne *et al.* [7] observed only simple surface dislocations, i.e., dislocations with unit Burgers vector. They found that the anchoring direction for the tilt plane is normal to the dislocation line. Since orientation of the tilt plane determines most optical properties of tilted smectic liquid crystals, the knowledge of the orientational action of dislocations on the director field is important for physics and applications of smectic structures. Observations of Galerne *et al.* [7] and Zhang *et al.* [1] stimulated our studies of dislocations in antiferroelectric liquid crystals.

In this paper we present investigations of orientational action of dislocations on the director field in antiferroelectric Smectic-C_A^* (SmC_A^*) freestanding films with two interfaces with air. In the SmC_A^* phase the direction of molecular tilt is opposite in nearest layers. Measurements were made in thin freestanding films with thickness from two to ten smectic layers. The thickness of the films is much less than the pitch of the smectic helix, so the orientation of the tilt plane in all layers of the film was practically the same. We find that orientation of the tilt plane depends uniquely on the parity of the normalized value of the Burgers vector $n = |\boldsymbol{b}|/d$. For odd n molecular tilt planes are parallel to the dislocation line on one side of the dislocation and perpendicular to it on the other side. For even n, orientations of the tilt plane on both sides are parallel to the dislocation axis. Unusual orientation for odd n can be associated with breaking of anticlinic symmetry which is realized if an odd number of layers are missing from one side of the dislocation. In this case the nearest two layers would have synclinic orientation (ferroelectric type) i.e., unfavorable for the antiferroelectric phase that leads to reorientation of the tilt plane in the perpendicular direction. The results of investigations are compared with orientation of the tilt plane near dislocations in ferroelectric liquid crystals.

II. EXPERIMENTAL DETAILS

In our investigations we used antiferroelectric SmC_A^* and ferroelectric SmC^* liquid crystals. The antiferroelectric liquid crystal was 4-(1-trifluoromethylheptyloxycarbonyl)phenyl 4′-octylbiphenyl-4-carboxylate (TFMHPBC) [9]. It exhibits the following phase sequence: SmC_A^*–(74.3 °C)–SmC_α^*–(75 °C)–SmA. In experiments with ferroelectric liquid crystal the mixture of nonpolar SmC and 83% ferroelectric SmC^* Felix-017/100 (AZ Electronic Materials) was used. This mixture has the ferroelectric phase at room temperature. For ferroelectric and antiferroelectric compounds two types of samples were used for investigations of director orientation by the edge dislocation. One was thin freestanding films (having thickness of two or three molecular layers) with islands of extra smectic layers. To obtain these samples the following method was used: A uniform thin film was prepared in a rectangular frame with two movable sides (metallic “blades”). After preparing the distance between metallic “blades” was rapidly decreased. The “blades” move so fast (with velocity about 3 cm/s) that the material of the thin film had no time to leave the film. Regions of larger thickness (circular islands) were formed in the film. The boundaries of the islands are edge dislocation. Samples of another type in our investigations were films with nonuniform thickness composed of regions with different numbers of layers which can be formed during preparation of the film. Experiments were performed using a custom-made heating stage. For SmC_A^* refractive index n_f of the film equals n_o for light polarization normal to the tilt plane and $n_f = n_{||}$ for light polarization parallel to the tilt plane. Films were imaged with a charge-coupled device (CCD) camera coupled to an Olympus BX51 microscope equipped with an Avantes fiber optic spectrometer. Thickness of the film was determined by measurements of intensity of reflection of nonpolarized light from the film [10]; see also Appendix A. Orientation of the tilt plane was determined by depolarized reflected light microscopy (DRLM) [11]; see also Appendix B.

III. DISLOCATIONS IN FERROELECTRIC FILMS

A typical DRLM image of a small and a large island in a SmC^* film is presented in Fig. 1(a). The boundary of an island is the edge dislocation. Previous studies [12–17] have shown that in SmC^* with a relatively large polarization, **c**-director configuration depends on island size. In small islands the configuration of the **c** director is circular. Large islands have a spiral texture. Such textures [Fig. 1(a)] and configuration of the director field [Figs. 1(b) and 1(c)] were also observed in our studies. The small island in the left-hand side of Fig. 1(a) has

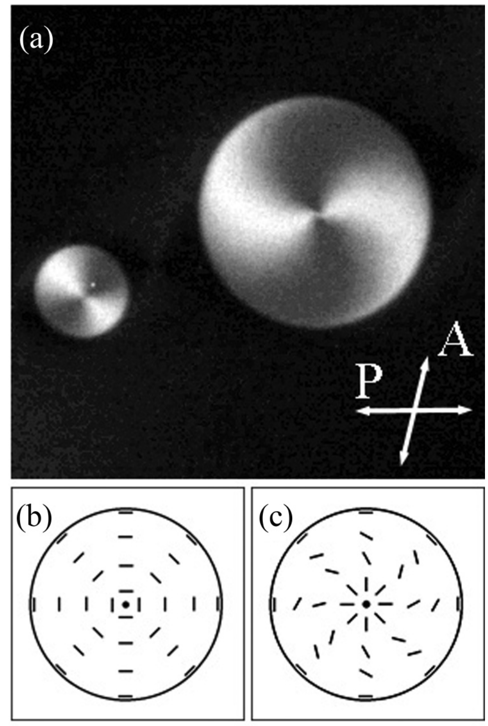

FIG. 1. Typical DRLM image of ferroelectric SmC^* islands in a thin SmC^* film (a) and sketches of director configuration in the islands (b,c). In small islands director configuration is circular (b), in large islands it is spiral (c). The orientation of the polarizer and the analyzer is shown in the lower right part of (a). The **c** director near the island boundary in the SmC^* film is parallel to the boundary of the island. $T = 25$ °C. The horizontal size of the photograph is 125 μm.

circular orientation of the director field [Fig. 1(b)]. The large island in the right-hand side of Fig. 1(a) has spiral configuration of the director field [Fig. 1(c)]. In all our experiments both in the circular and spiral configuration the tilt plane was parallel to the boundary of islands, that is, parallel to the edge dislocation. This is consistent with previous optical observations [12–17].

In order to confirm this result for films composed of regions with different number of layers we made investigations of director orientation in such SmC^* films. Figure 2 shows the DRLM images of ferroelectric films with regions of different thickness. Borders between regions with different numbers of layers are shown by arrows. These boundaries are the edge dislocations. Numbers in the frames denote the number of layers in the corresponding region of the film. The difference between the number of layers is the normalized value of Burgers vector $n = |\boldsymbol{b}|/d$. The dislocations in the central part of the photo are oriented approximately at an angle of 45° with respect to the polarizer. So, DRLM allows us to determine the orientation of the director field. Figure 2(a) shows a film with π walls (black stripes) oriented nearly perpendicular to dislocation lines. The film is bright near the dislocations which for our orientation of the polarizer and the analyzer indicates that the tilt planes are oriented parallel to the dislocation (short lines near the dislocations show the orientation of the **c** director). Brightness near the dislocations corresponds to Fig. 12(a) in Appendix B. The **c**-director orientation on the two sides of the π wall is opposite, but the tilt plane remains parallel

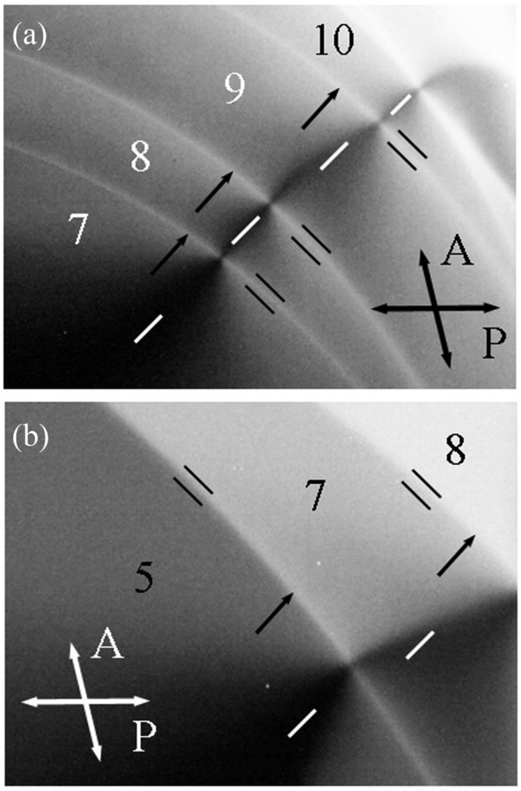

FIG. 2. Ferroelectric SmC^* film with a step-by-step increase of thickness by elementary edge dislocations with $|\boldsymbol{b}| = d$ (a). A dislocation with vector $|\boldsymbol{b}| = 2d$ is present in (b). The layer steps are shown by arrows. Numbers denote the number of molecular layers in the different regions of the film. Orientations of the tilt planes are parallel to the edge dislocations regardless of the value of the Burgers vector and are shown by short lines. DRLM; bright regions of the films near the dislocations correspond to orientation of the tilt plane shown in Fig. 12(a) in Appendix B. The horizontal size of the image is 331 μm. $T = 21\,^{\circ}$C.

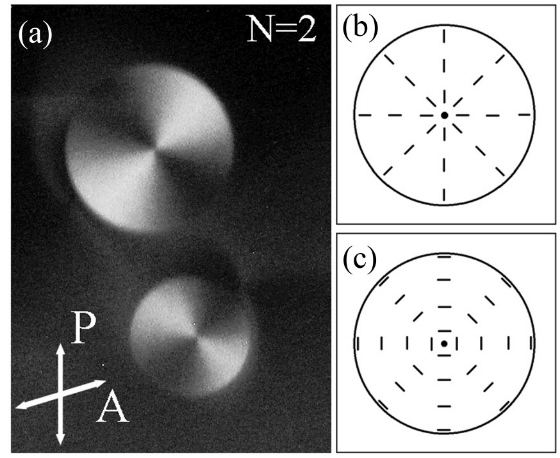

FIG. 3. DRLM image of antiferroelectric SmC_A^* islands (a). Dark regions are located in different parts of two islands. (b,c) show the orientation of the tilt plane correspondingly in the upper and lower islands in (a). The **c** director near the island boundary in the SmC_A^* films can be perpendicular and parallel (b,c) to the boundary of the island. Dark and bright regions in the islands correspond to orientation of the tilt plane depicted in Figs. 12(e) and 12(f) in Appendix B. The horizontal size of the photo is 182 μm. $T = 62\,^{\circ}$C.

to the dislocation line. In Fig. 2(a) steps between regions of different thickness are elementary dislocations. Figure 2(b) shows an elementary dislocation and a dislocation with an even value of Burgers vector. In ferroelectric films with dislocations and in films with islands regardless of the number of layers and of the value of Burgers vector we observed the orientation of the **c** director parallel to the dislocation line.

IV. DISLOCATIONS IN ANTIFERROELECTRIC FILMS

Now we study in detail the orientation of the **c**-director near edge dislocations in antiferroelectric SmC_A^* films. We start with films with smectic islands. The orientation of the **c** director in the SmC_A^* can differ drastically in different islands [Fig. 3(a)]. Bright and dark brushes orient perpendicularly in the two islands in Fig. 3(a). Rotation of the film does not change the orientation of dark and bright areas. DRLM images of islands indicate that the tilt plane in the islands has C_∞ symmetry but can be both parallel and perpendicular to the island boundary for islands in the same film. Figures 3(b) and 3(c) show the orientation of the tilt plane in islands located in the upper and lower part of Fig. 3(a). Examination of the image obtained using DRLM [see Appendix B, Figs. 12(e) and 12(f)] reveals that the **c** director is parallel to the boundary in the island in the lower part of Fig. 3(a) and perpendicular to the boundary in the island in the upper part of Fig. 3(a). This behavior is significantly different from orientation of the **c** director near the boundary of SmC^* islands, that is, near edge dislocations in the ferroelectric SmC^* films.

Our finding is that the relative orientation of the **c** director on two sides of the dislocation depends on the value of the Burgers vector of the dislocation. Figure 4 shows samples consisting of several regions with an odd number of layers [Fig. 4(a)] and with an even number of layers [Fig. 4(b)]. In both cases the normalized values of Burgers vector $n = |\boldsymbol{b}|/d$ are even ($n = 2$ or $n = 4$). Comparing the darkness of the images near edge dislocations with darkness near line stripes (e.g., near a 2π wall in the seven-layer film) indicates that regions near two sides from edge dislocations in Fig. 4(a) are bright. In the DRLM geometry of Fig. 4(b) regions near the edge dislocation appear dark. The edge dislocation is shown by an arrow. Examination of DRLM texture [see Appendix B, Figs. 12(a) and 12(c)] shows that near dislocations in all films in Fig. 4 whose thickness differs by an even number of molecular layers the orientation of the **c** director is parallel to the dislocation line.

Now we consider the dislocations with odd normalized values of Burgers vector n. Figure 5 shows examples of such samples composed of two regions of the film whose thickness differs by one layer [five-layer and six-layer regions in Fig. 5(a), four-layer and three-layer regions in Fig. 5(b)]. Double dark and bright stripes in the photos are 2π walls. In DRLM geometry of Fig. 5 bright regions correspond to the tilt plane parallel to the dislocation line; dark regions correspond to tilt plane orientation perpendicular to the dislocation line. We can see that the orientation of the tilt plane on two sides of the dislocation is mutually perpendicular [the **c** director is parallel to the layer step in the five-layer film and

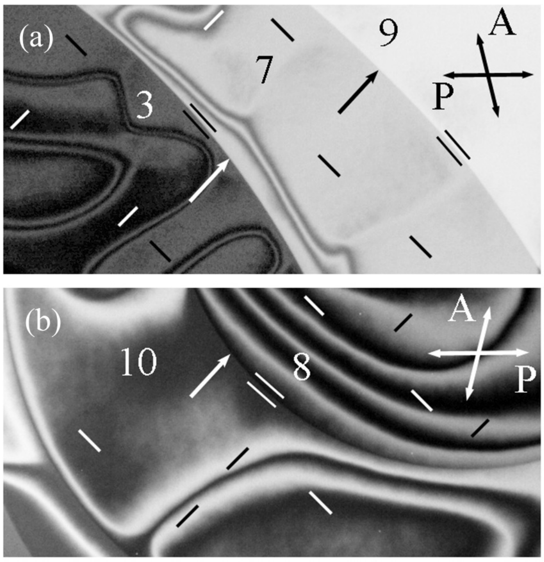

FIG. 4. DRLM images of antiferroelectric SmC_A^* films with edge dislocations. Numbers denote the number of molecular layers in different regions of the film. Their thickness differs by an even number of layers. Dislocations are shown by arrows. Orientation of the tilt plane near edge dislocation is parallel to the dislocation and is shown by short lines. In frame (a) the bright regions near the dislocations correspond to Fig. 12(a) in Appendix B; in panel (b) the dark region near the dislocation corresponds to Fig. 12(c) in Appendix B. The horizontal size of the images is 550 μm (a) and 331 μm (b). $T = 60\,^{\circ}$C.

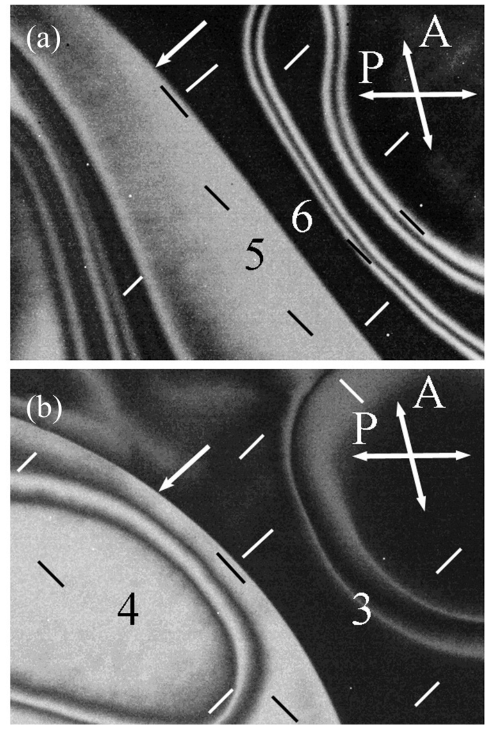

FIG. 5. DRLM images of antiferroelectric SmC_A^* films with two regions which differ in thickness by one smectic layer. The number of molecular layers is denoted in each region of the films. The elementary edge dislocations separate bright and dark areas and are shown by arrows. Tilt planes on the two sides from the dislocation are perpendicular and are shown by short lines. Double dark and bright stripes are 2π walls. The bright region near the dislocation corresponds to Fig. 12(a) in Appendix B for the five-layer film and for the four-layer film; the dark region near the dislocation corresponds to Fig. 12(b) in Appendix B for the six-layer film and for the three-layer film. The horizontal size of the images is 497 μm (a) and 663 μm (b). $T = 60\,^{\circ}$C.

perpendicular in the six-layer film, Fig. 5(a); in Fig. 5(b) the **c** director is parallel to the layer step in the four-layer film and perpendicular in the three-layer film]. The same mutually perpendicular orientation of the tilt plane is observed near dislocations with larger odd values of the normalized Burgers vector. Figure 6 shows SmC_A^* samples consisting of regions which differ in thickness by three layers [Fig. 6(a)] and five layers [Fig. 6(b)]. In the three-layer and five-layer films the tilt plane is perpendicular to the dislocation; in the six-layer and ten-layer films it is parallel to the dislocation. We observed such mutually perpendicular orientation in TFMHPBC films with thickness up to ten layers and dislocations with odd normalized Burgers vector up to five.

Perpendicular orientation of the **c** director on different sides of the dislocation was not observed before, both in nonpolar SmC and in polar SmC^* and SmC_A^* films. In order to confirm this unusual orientational action of edge dislocations we performed measurements using another optical method. In Fig. 7 the dislocation divides parts of the film with six and seven layers. Measurements were made in linearly polarized light (without an analyzer) with direction of polarization nearly perpendicular to the dislocation. As $n_\parallel > n_o$ (see Appendix B), in parts of the film with uniform thickness (six layers or seven layers in Fig. 7) brighter regions correspond to **c**-director orientation parallel to the polarizer. In dark regions **c**-director orientation is perpendicular to the polarization of light. Orientation of the tilt planes in dark and bright regions is shown by short lines. It is clear from Fig. 7 that the dislocation orients the **c** director parallel to the dislocation line in the six-layer region and perpendicular to it in the seven-layer region. Similar measurements were made for dislocations with even values of the normalized Burgers vector n. Figure 8 shows a film consisting of regions with four and six layers. Large reflected intensity near the dislocation with respect to reflection from two stripes of 2π walls indicates that the **c** director orients parallel to the dislocation line. The performed measurements (Figs. 4–8) show that the orientation of the **c** director does not depend on film thickness; the mutual orientation of the **c** director on two sides from the dislocation depends on the value of the Burgers vector.

V. DISCUSSION AND SUMMARY

We found that layer-by-layer alternation of the molecular tilt in antiferroelectric SmC_A^* imposes restrictions on the orientation of the molecular tilt around the dislocation. Now we may speculate about the possible reason for the observed phenomena, in particular, the reason for the perpendicular orientation of the tilt plane on two sides of the dislocation with odd n.

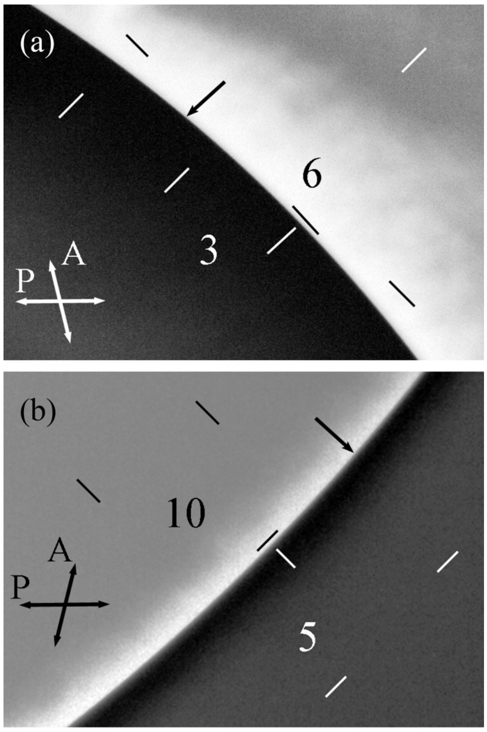

FIG. 6. DRLM images of antiferroelectric films with regions which differ in thickness by three and five smectic layers. The number of molecular layers is indicated in each region of the films. Edge dislocations are denoted by arrows. Orientation of the tilt plane in the darkest and brightest region of the film is shown by short lines. The orientation of the tilt planes on two sides of the dislocations is mutually perpendicular. In (a) brightness near the dislocation corresponds to Fig. 12(a) in Appendix B for the six-layer film and to Fig. 12(b) in Appendix B for the three-layer film. In (b) brightness near the dislocation corresponds to Fig. 12(c) in Appendix B for the five-layer film and to Fig. 12(d) in Appendix B for the ten-layer film. The horizontal size of the images is 253 μm (a) and 166 μm (b). $T = 59\,^{\circ}$C.

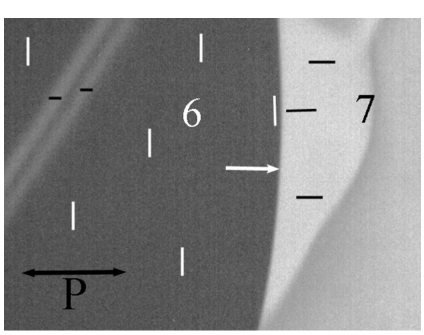

FIG. 7. Antiferroelectric SmC_A^* film with an edge dislocation. The photograph was taken in linearly polarized light. Direction of light polarization is shown in the lower part of the image. Orientation of the tilt plane is perpendicular in the regions near the dislocation in films of different thickness. The horizontal size of the image is 249 μm.

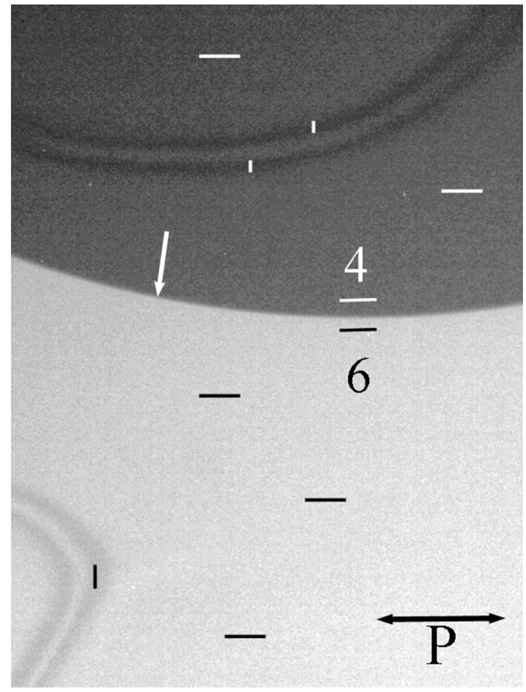

FIG. 8. Antiferroelectric film with two regions of an even number of layers. The dislocation is shown by an arrow. The photograph was taken in linearly polarized light. Orientation of the tilt plane in the region near the dislocation is parallel to the dislocation. The horizontal size of the image is 249 μm. $T = 60\,^{\circ}$C.

Let us consider first a film with an odd value of the normalized value of Burgers vector (e.g., an elementary dislocation with $n = 1$). Figure 9(a) shows a film with an even number of layers ($N = 4$). Creation of an elementary dislocation can be considered as a process in which one layer is added in the left-hand part of the film [Fig. 9(b)]. Now in the five-layer region [left part of Fig. 9(b)] the two nearest layers have synclinic orientation of the tilt direction (these layers are marked gray). A synclinic pair of layers will also be present for the opposite orientation of the **c** director in the added layer. The same tilt direction in the nearest layers leads to breaking of antiferroelecrtic ordering in the left-hand region of the film. Synclinic orientation is unfavorable. Exit from this frustration can be the reorientation of the tilt planes so that they become perpendicular to the dislocation line and have anticlinic ordering [Fig. 9(c)]. A synclinic pair will also appear if one layer is removed from an antiferroelectric film [Fig. 10(b), two gray layers]. In this case frustration [Fig. 10(b)] and reorientation of tilt planes perpendicular to the dislocation line occur in the region of the film with an even number of layers [Fig. 10(c)]. We observed both situations with the tilt plane perpendicular to the dislocation in regions of the film with odd and even number of layers (Figs. 5 and 6). In films with the same parity of number of layers on two sides from the dislocation (i.e., with n-even dislocations) the orientation of the **c** director remains anticlinic as two layers with opposite orientation of the **c** director are added or removed. Ferroelectric pairs are not formed [Figs. 11(a) and 11(b)]. In this case the tilt planes remain parallel to the dislocation line [Fig. 11(b)]. The present model of mixed anchoring can describe the

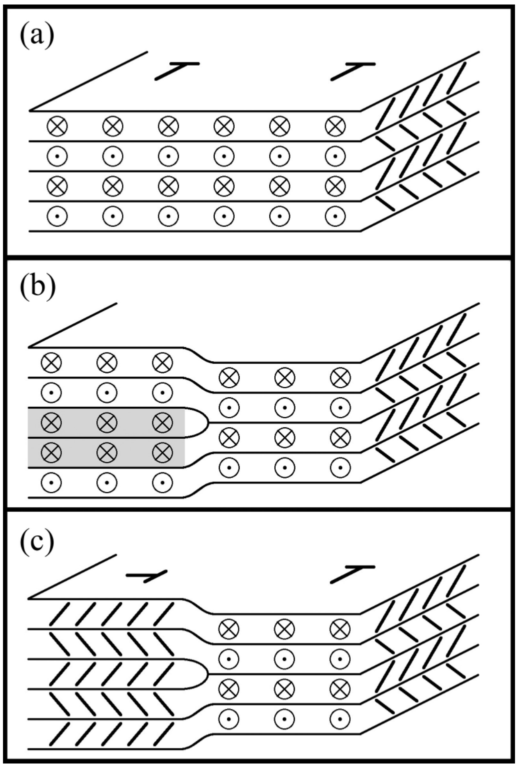

FIG. 9. Schematic representation of a four-layer freestanding antiferroelectric SmC_A^* film (a). Molecular orientation is shown in each layer. Panel (b) shows a film with a dislocation; one layer is added in the left part of the film. A ferroelectric pair is formed in the interior of the film (b) which breaks the antiferroelectric ordering. The ferroelectric pair is shown by gray. The orientational structure is transformed in the left part of the film and tilt planes on two sides from the dislocation become perpendicular (c). Orientation of the **c** director in the top layers of the films is shown by nails.

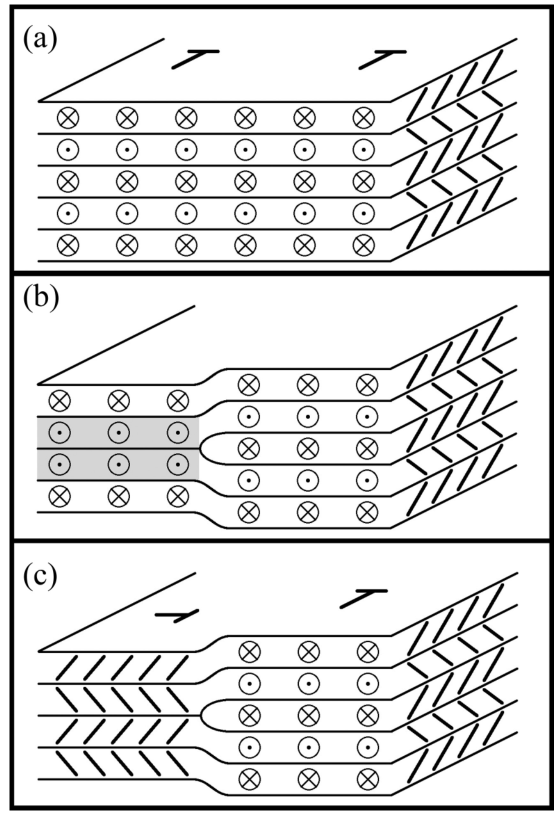

FIG. 10. Schematic representation of a five-layer freestanding antiferroelectric film (a). Molecular orientation is shown in each layer. Panel (b) shows a film with a dislocation; one layer is removed in the left part of the film. A ferroelectric pair is formed in the interior of the film (b) which breaks the antiferroelectric ordering. The ferroelectric pair is shown by gray. The orientational structure is transformed in the left part of the film and tilt planes on two sides from the dislocation become perpendicular (c).

experiment for thin films (nanofilms). It is worth noting, however, that this model is a hypothesis which correlates with observations. Further theoretical studies are needed for a clear understanding of the nature of orientational action of dislocations. In thick films the situation can be more complex than in nanofilms including moving the dislocation with a synclinic pair to the surface. Study of orientational action of dislocations in thick films is a subject of future investigations. Note that in bulk samples of antiferroelectric liquid crystals dispirations can exist, which combine a disclination line and a dislocation [18,19]. In thin freestanding films free surfaces do not restrict **c**-director orientation, and dispirations are not realized.

The question arises, what is the orientation of polarization near a dislocation? We remind the reader that in odd-layer SmC_A^* films the net polarization of the film is perpendicular to the tilt plane; in even-layer films it is parallel to the tilt plane [20,21]. Taking into account the orientation of polarization with respect to the tilt plane it is clear from Figs. 4–8 that polarizations on two sides of the dislocation line are collinear in all films. Note that there are two preferred orientations of polarization near a layer step. The polarization can be parallel or perpendicular to the dislocation [Figs. 4(a), 4(b), 5(a), and 5(b)].

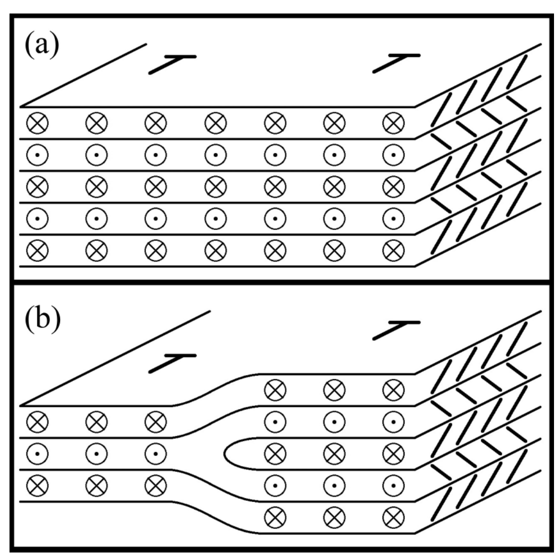

FIG. 11. Schematic representation of a five-layer freestanding antiferroelectric film (a). Molecular orientation is shown in each layer. Frame (b) shows a film with a dislocation: two layers are removed in the left part of the film. A dislocation with the Burgers vector $|\boldsymbol{b}| = 2d$ (b) does not induce a ferroelectric pair. Tilt planes remain parallel on two sides from the dislocation.

As we mention in the Introduction, Zhang *et al.* [1] observed in ferroelectric films dislocations of so-called A type where the **c** director on both sides of the dislocation is perpendicular to it. Previous studies as well as the results reported in this work show that in nonpolar SmC and in SmC^* preferential orientation of the **c** director on two sides of edge dislocations in freestanding films is parallel to the dislocation [13–17,22–26]. A possible reason for this preferential orientation was described by Hatwalne and Lubensky [27]. They indicated that an edge dislocation with its core parallel to the **c** director has a lower energy with respect to a dislocation with its core perpendicular to the **c** director. The possible reason that dislocations of A type are not observed in freestanding films is that in freestanding films molecular orientation in the film planes can change and choose the configuration with the least energy. Another reason may be that in the investigations of Zhang *et al.* the smectic sample was quenched in liquid nitrogen and its thickness was fixed; meanwhile we investigated freestanding smectic films. An interesting observation regarding dislocations in freestanding films was made by Link *et al.* [20]. They reported that in inhomogeneous SmC_A^* films regions of different thickness tend to segregate according to the parity of the number of layers, resulting in regions of odd and even layer numbers. This may indicate that the preferred value of normalized Burgers vector n in SmC_A^* films is a multiple of 2.

In summary, we studied the orientation of the **c** director near layer steps (edge dislocations) in freestanding films of antiferroelectric SmC_A^* liquid crystal. We found that the orientation of the **c** director can be different and depends on the Burgers vector of the dislocation. Near dislocations with Burgers vector corresponding to an even number of layers the **c**-director is aligned parallel to the layer step. Near dislocations with Burgers vector equal to an odd number of layers the mutual orientation of the **c** director on two sides of the dislocation is perpendicular. We discuss that a possible origin of this phenomenon is related to layer-by-layer alternation of molecular orientation in antiferroelectric films. Interplay of energy of an edge dislocation and orientation of the **c** director near the dislocation can result in nontrivial orientational structures near dislocations in antiferroelectric films.

ACKNOWLEDGMENTS

The reported study was supported in part by RFBR, Project No. 16-29-11702. We thank Showa Shell Sekiyu K.K. for supplying the liquid-crystal compound TFMHPBC.

APPENDIX A: DETERMINATION OF FILM THICKNESS

Reflectivity R of a film depends on the refractive index n_f in the plane of the film [10,28],

$$R = \frac{\left(n_f^2 - 1\right)^2 \sin^2(2\pi n_f N d/\lambda)}{4n_f^2 + \left(n_f^2 - 1\right)^2 \sin^2(2\pi n_f N d/\lambda)}, \qquad \text{(A1)}$$

$R = I/I_0$, where I_0 and I are the intensities of the incident and reflected light, respectively; λ is the wavelength of light in vacuum. For thin films (A1) can be rewritten as

$$R \approx \left[\pi N d\left(n_f^2 - 1\right)/\lambda\right]^2. \qquad \text{(A2)}$$

The quadratic dependence of R on N for thin films enables us to determine the number of layers without knowing n_f and d. First, several thin films of different thickness are prepared and their reflectivity is measured. The number of layers in each film can be determined comparing the ratios of reflected intensities with ratios of different integers squared [see Eq. (A2)]. After the reflectivity values for several thicknesses are known, we are able to determine the number of layers in a prepared film from its reflectivity.

APPENDIX B: DEPOLARIZED REFLECTED LIGHT MICROSCOPY (DRLM)

To make the discussion of experimental results easier, let us recall the principles of DRLM [11,20,29,30]. A smectic film in the SmC^* or SmC_A^* phase is optically anisotropic. For elongated molecules of TFMHPBC type the refractive index in the direction parallel to the tilt plane $n_\parallel$ is larger than in the direction perpendicular to the tilt plane n_o (see, e.g., [21]). Linearly polarized light is incident on the film. For thin films reflected intensity of light polarized parallel to the tilt plane is larger than that for polarization perpendicular to

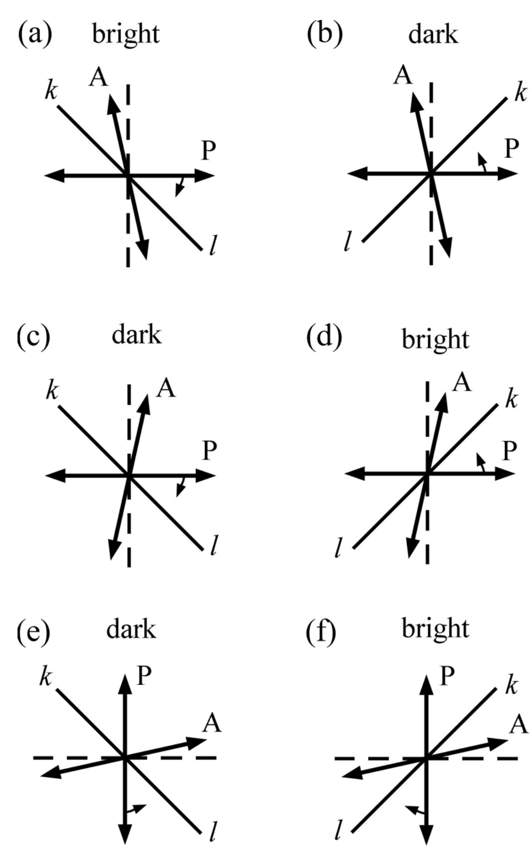

FIG. 12. (a–f) illustrate different orientations of the polarizer (P) and the analyzer (A) with respect to the tilt plane kl in DRLM geometry. Words “bright” and “dark” describe the appearance of films in the regions where the tilt plane is parallel to the line kl. The curved arrow in each panel shows the direction of the effective rotation of the plane of polarization of light reflected from the film.

the tilt plane because $n_{\parallel} > n_o$ [see Eq. (A2), where $n_f = n_{\parallel}$ or n_o]. Figures 12(a)–12(f) demonstrate different orientations of the polarizer with respect to molecular tilt plane kl. If the incident light polarization is oriented under 45° with respect to the tilt plane, the plane of polarization of reflected light effectively rotates towards the tilt plane [20,29,30]. The curved arrow in each frame shows the direction of the effective rotation of the plane of polarization of light reflected from the film. Decrossing of the analyzer under an appropriate angle discriminates regions with orientation of the tilt plane at the angle of +45° and of −45° with respect to the polarizer. One of the regions becomes darker, and the other one brighter. In order to demonstrate clearly which region is darker or brighter we show in this paper photos of the films with orientational defects (e.g., 2π walls [20,31,32]) in which there are dark and bright stripes. Large optical contrast in DRLM is achieved due to difference of refractive index parallel and perpendicular to the tilt plane. In our studies DRLM measurements were made in white light and using a color filter. Both measurements gave the same results. DRLM can be used independently of curvature of dislocations and splay-bend energy.

[1] C. Zhang, A. M. Grubb, A. J. Seed, P. Sampson, A. Jakli, and O. D. Lavrentovich, Nanostructure of Edge Dislocations in a Smectic-C^* Liquid Crystal, Phys. Rev. Lett. **115**, 087801 (2015).
[2] M. Maaloum, D. Ausserre, D. Chatenay, G. Coulon, and Y. Gallot, Edge Profile of Relief 2D Domains at the Free Surface of Smectic Copolymer Thin Films, Phys. Rev. Lett. **68**, 1575 (1992).
[3] J. A. Collett and D. M. Zambrano, Using dislocations to probe surface reconstruction in thick freely suspended liquid crystalline films, Phys. Rev. E **92**, 040501(R) (2015).
[4] R. B. Meyer, B. Stebler, and S. T. Lagerwall, Observation of Edge Dislocations in Smectic Liquid Crystals, Phys. Rev. Lett. **41**, 1393 (1978).
[5] P. G. de Gennes and J. Prost, *The Physics of Liquid Crystals*, 2nd ed. (Clarendon Press, Oxford, 1995).
[6] Y. Galerne and L. Liebert, Smectic-*O* Films, Phys. Rev. Lett. **64**, 906 (1990).
[7] V. Candel and Y. Galerne, Anchoring Strength onto Simple Surface Edge Dislocations in an Induced Smectic-*O* Film, Phys. Rev. Lett. **70**, 4083 (1993).
[8] P. Oswald and P. Pieranski, *Smectic and Columnar Liquid Crystals: Concepts and Physical Properties Illustrated by Experiments* (Taylor & Francis, London, 2006).
[9] A. Fukuda, Y. Takanishi, T. Isozaki, K. Ishikawa, and H. Takezoe, Antiferroelectric chiral smectic liquid crystals, J. Mater. Chem. **4**, 997 (1994).
[10] P. Pieranski, L. Beliard, J.-Ph. Tourellec, X. Leoncini, C. Furtlehner, H. Dumoulin, E. Riou, B. Jouvin, J. P. Fénerol, Ph. Palaric, J. Hueving, B. Cartier, and I. Kraus, Physics of smectic membranes, Physica A **194**, 364 (1993).
[11] D. R. Link, G. Natale, R. Shao, J. E. Maclennan, N. A. Clark, E. Korblova, and D. M. Walba, Spontaneous formation of macroscopic chiral domains in a fluid smectic phase of achiral molecules, Science **278**, 1924 (1997).
[12] R. B. Meyer, D. Konovalov, I. Kraus, and J.-B. Lee, Equilibrium size and textures of islands in free-standing smectic C* films, Mol. Cryst. Liq. Cryst. **364**, 123 (2001).
[13] J.-B. Lee, D. Konovalov, and R. B. Meyer, Textural transformations in islands on free standing smectic-C^* liquid crystal films, Phys. Rev. E **73**, 051705 (2006).
[14] J.-B. Lee, R. A. Pelcovits, and R. B. Meyer, Role of electrostatics in the texture of islands in free-standing ferroelectric liquid crystal films, Phys. Rev. E **75**, 051701 (2007).
[15] A. Pattanaporkratana, C. S. Park, J. E. Maclennan, and N. A. Clark, Direct measurement of interaction forces between islands on freely suspended smectic C films using multiple optical tweezers, Ferroelectrics **344**, 71 (2006).
[16] P. V. Dolganov and P. Cluzeau, Manifold configurations of the director field formed by topological defects in free and confined geometry in smectic films, Phys. Rev. E **90**, 062501 (2014).
[17] P. V. Dolganov, N. S. Shuravin, V. K. Dolganov, and E. I. Kats, Topological defects in smectic islands in freely suspended films, Pis'ma v ZhETF **101**, 505 (2015) [JETP Lett. **101**, 453 (2015)].
[18] Y. Takanishi, H. Takezoe, A. Fukuda, and J. Watanabe, Visual observation of dispirations in liquid crystals, Phys. Rev. B **45**, 7684 (1992).
[19] K. Miyachi, Y. Takanishi, K. Ishikawa, H. Takezoe, and A. Fukuda, Does the disclination line exist in a homogeneously aligned SmC_A^* cell? Ferroelectrics **149**, 61 (1993).
[20] D. R. Link, J. E. Maclennan, and N. A. Clark, Simultaneous Observation of Electric Field Coupling to Longitudinal and Transverse Ferroelectricity in a Chiral Liquid Crystal, Phys. Rev. Lett. **77**, 2237 (1996).
[21] P. V. Dolganov, Y. Suzuki, and A. Fukuda, Structural transitions in thin free-standing films of an antiferroelectric liquid crystal exhibiting the smectic-C_α^* phase in the bulk sample, Phys. Rev. E **65**, 031702 (2002).
[22] C. Völtz and R. Stannarius, Self-organization of isotropic droplets in smectic-*C* free-standing films, Phys. Rev. E **70**, 061702 (2004).
[23] D. Pociecha, E. Gorecka, N. Vaupotič, M. Čepič, and J. Mieczkowski, Spontaneous Breaking of Minimal Surface Condition: Labyrinths in Free Standing Smectic Films, Phys. Rev. Lett. **95**, 207801 (2005).
[24] P. V. Dolganov and P. Cluzeau, Influence of chirality on director configuration and droplet interaction in ferroelectric free-standing films, Phys. Rev. E **78**, 021701 (2008).
[25] N. M. Silvestre, P. Patricio, M. M. Telo da Gama, A. Pattanaporkratana, C. S. Park, J. E. Maclennan, and N. A. Clark, Modeling dipolar and quadrupolar defect structures generated by chiral islands in freely suspended liquid crystal films, Phys. Rev. E **80**, 041708 (2009).
[26] A. Eremin, U. Kornek, R. Stannarius, W. Weissflog, H. Nádasi, F. Araoka, and H. Takezoe, Labyrinthine instability in freely suspended films of a polarization-modulated smectic phase, Phys. Rev. E **88**, 062512 (2013).
[27] Y. Hatwalne and T. C. Lubensky, Covariant elasticity and dislocations in smectic-C liquid crystals, Phys. Rev. E **52**, 6240 (1995).

[28] M. Born and E. Wolf, *Principles of Optics* (Pergamon, New York, 1964).

[29] R. Pindak, C. Y. Young, R. B. Meyer, and N. A. Clark, Macroscopic Orientation Patterns in Smectic-C Films, Phys. Rev. Lett. **45**, 1193 (1980).

[30] A. Eremin, A. Nemeş, R. Stannarius, and W. Weissflog, Ambidextrous bend patterns in free-standing polar Smectic-CP_F films, Phys. Rev. E **78**, 061705 (2008).

[31] P. V. Dolganov, B. M. Bolotin, and A Fukuda, 2π and π walls in antiferroelectric smectic-C_A^* and smectic-C free-standing films, Phys. Rev. E **70**, 041708 (2004).

[32] N. Chattham, M.-G. Tamba, R. Stannarius, E. Westphal, H. Gallardo, M. Prehm, C. Tschierske, H. Takezoe, and A. Eremin, Leaning-type polar smectic-C phase in a freely suspended bent-core liquid crystal film, Phys. Rev. E **91**, 030502(R) (2015).